




Article

RF Fingerprinting Using Transient-Based Identification Signals at Sampling Rates Close to the Nyquist Limit

Selçuk Taşcıoğlu ¹, Aykut Kalaycıoğlu ^{1,*}, Memduh Köse ² and Gokhan Soysal ¹

¹ Department of Electrical and Electronics Engineering, Ankara University, Ankara 06830, Türkiye; selcuk.tascioglu@eng.ankara.edu.tr (S.T.); soysal@eng.ankara.edu.tr (G.S.)

² Department of Electrical and Electronics Engineering, Kırşehir Ahi Evran University, Kırşehir 40100, Türkiye; memduh.kose@ahievran.edu.tr

* Correspondence: kalaycioglu@ankara.edu.tr

Abstract: Radio frequency (RF) fingerprinting is regarded as a promising solution to improve wireless security, especially in applications where resource-limited devices are employed. Unlike steady-state signals, such as preambles or data, the use of short-duration transient signals for RF fingerprinting offers distinct advantages for systems with low latency and low complexity requirements. One of the challenges associated with transient-based methods in practice is achieving high performance while utilizing low-cost receivers. In this study, we demonstrate for the first time that the performance of transient-based RF fingerprinting can be enhanced by designing the filter chain in a software defined radio (SDR) receiver, taking into account the relevant signal characteristics. The performance analysis is conducted using transient-based identification signals captured by the SDR receiver, focusing on the sampling rate and duration of the identification signal. In the experiments, signals collected from twenty IEEE 802.11 transmitters are used. Experimental results indicate that so long as the receiver filter parameters and the duration of the identification signal are properly determined, a high classification performance exceeding 92% can be achieved for transient-based RF fingerprinting, even at sampling rates approaching the Nyquist limit.

Keywords: designing filter chain; duration of identification signal; RF fingerprinting; SDR receiver; transient signals



Academic Editors: Yanjun Pan, Yao Zheng and Shangqing Zhao

Received: 23 November 2024

Revised: 18 December 2024

Accepted: 22 December 2024

Published: 24 December 2024

Citation: Taşcıoğlu, S.; Kalaycıoğlu, A.; Köse, M.; Soysal, G. RF Fingerprinting Using Transient-Based Identification Signals at Sampling Rates Close to the Nyquist Limit. *Electronics* **2025**, *14*, 4. <https://doi.org/10.3390/electronics14010004>

Copyright: © 2024 by the authors. Licensee MDPI, Basel, Switzerland. This article is an open access article distributed under the terms and conditions of the Creative Commons Attribution (CC BY) license (<https://creativecommons.org/licenses/by/4.0/>).

1. Introduction

With the widespread use of wireless communication systems in a large number of applications, such as autonomous vehicles and unmanned aerial vehicles in both civil and military fields, the issue of improving wireless security has become more important. The conventional password-based security systems are vulnerable to being copied and cracked by third-party users; moreover, in low-cost systems, complex security mechanisms such as cryptography cannot be directly applied to mobile devices due to their limited energy and computing resources [1]. In addition, ensuring wireless security while meeting the criteria of low power and resource consumption in critical applications is essential. Thus, a physical layer network security method based on radio frequency (RF) fingerprinting is a candidate solution for such purposes. RF fingerprints are unique characteristics of wireless transmitters that are embedded in the transmission signals due to effects of physical layer hardware imperfections. These characteristics can be obtained from the transient, preamble, or data signal regions to identify the wireless devices. The physical layer fingerprints have hardware-specific properties and are hard to mimic, making them be robust [2].

Since RF fingerprints, carrying unique characteristics of the wireless transmitters while broadcasting, are embedded directly into the transmission signals, identification of the transmitters does not require any additional hardware or computational load. In this respect, RF fingerprinting-based solutions are suitable and promising wireless security methods for mobile devices that are limited in terms of power and computational resources.

In earlier studies, RF fingerprinting-based solutions relied on the use of high-cost receivers [3–6], which was a limiting factor for the widespread implementation of these methods in practical applications. The proliferation of low-cost receivers has led to a significant rise in the number of studies employing RF fingerprinting techniques for signals acquired through these devices. Numerous studies have demonstrated that high classification performance can be achieved with low-cost receivers where fingerprints are commonly obtained from the long duration preamble signal region [7–11]. On the other hand, as reported in a recent survey [2], few studies in the literature have employed low-cost receivers for transient-based RF fingerprinting. In fact, in systems with low complexity and low latency requirements [12], transient-based methods offer significant advantages. Namely, these techniques utilize short identification signals at the beginning of transmissions, resulting in lower latency compared to steady-state approaches. In addition, these techniques do not need any prior knowledge of the wireless communication standard, nor do they require demodulation of signals [13]. Thus, they also have the advantage of being computationally efficient.

The sampling rate of the receiver is one of the important parameters that should be considered for RF fingerprinting-based identification, as discussed in recent studies [2,14–16]. Low-cost receivers have much lower sampling rates, typically in the order of megasamples per second (MS/s), compared to high-end receivers. Although the effect of sampling rate on classification performance has been discussed for steady-state approaches [4,8], a comprehensive discussion is necessary for transient-based techniques. In the literature, few studies have investigated the effect of sampling rates on the transient-based approach using high-end receivers. For instance, in [4], a high-end receiver system having a spectrum analyzer and an oscilloscope with a sampling rate of 4 GS/s was used to investigate this effect. The minimum sampling rate was taken as 32 times the transmission bandwidth, which is quite high for analyzing large-bandwidth signals in a low-cost receiver system. Another study [17], also using a high-end receiver with a 5 GS/s sampling rate, showed that reducing the sampling rate via decimation in post-processing did not significantly affect the transient-based classification performance. Although the performance of transient-based RF fingerprinting has been discussed with low sampling rates by decimating the signals captured by high-end receivers, demonstrating their usability in low-cost receiver systems operating at low sampling rates is critical. This is because the signal capturing hardware directly influences the classification performance [18].

Although transient signals have considerably shorter durations compared to the steady-state signals, they contain tremendous descriptive information and are more distinctive [19,20]. To obtain this descriptive information from transmitted signals without loss, the duration of the identification signal containing transients should be carefully determined. In the literature, [6] emphasizes the importance of accurately determining transient duration on the performance for a high-end receiver system. In a recent study [21], for identification signals including the steady-state portion, the authors indicated that more information about fingerprints can be obtained by data augmentation. In addition, they also mentioned that directly increasing the signal duration or sampling rate would likely be a more effective way under suitable conditions. Thus, the duration of the transient-based identification signals should also be discussed to analyze the classification performance of the RF fingerprinting using these signals for low-cost receivers.

The noise level in signals captured with low-cost receivers may be higher compared to high-end receivers, so reducing the distorting effects in low-cost receivers is essential for RF fingerprinting performance [22]. In [8], the noise introduced by low-cost analog components was reduced using signal processing tools in a computer environment after the data collection phase, which is called post-collection signal processing. In that study, signals transmitted from IEEE 802.15.4 devices were collected with low-cost receivers, and a preamble-based method was employed for classification. In transient-based methods, the adverse effects of noise may be more pronounced due to the limited number of samples available for identification. In [13], a smoothing algorithm that reduces the noise effect was proposed in order to increase the performance of transient-based fingerprints obtained from the ZigBee devices.

In this study, we aim to reduce noise by designing the filter chain in a low-cost receiver in accordance with the spectral characteristics of transmitted signals, while also enabling high out-of-band rejection at the data acquisition step. Consequently, unlike the methods that reduce noise through post-collection signal processing, the proposed approach does not introduce any additional processing associated with noise reduction for RF fingerprinting. Additionally, unlike previous studies that examined the effect of sampling rate with high-end receivers, we focus on a transient-based approach at low sampling rates, particularly using a low-cost receiver. The impact of the designed receiver filters on classification performance is analyzed for various sampling rates and two SNR levels. Additionally, the effect of the duration of the identification signal, an important parameter influencing RF fingerprinting performance, is examined, even though the design of the receiver filter is independent of this parameter. In the experiments, signals collected from twenty Wi-Fi transmitters are used. As a result, we show that transient-based RF fingerprinting can be effectively employed at sampling rates approaching the Nyquist limit so long as the receiver filter parameters and the duration of the identification signal are properly determined.

The main contributions of this study can be summarized as follows. To the best of our knowledge, the following aspects are considered for the first time:

- We demonstrate that the performance of RF fingerprinting can be enhanced by designing the filter chain in an SDR receiver, taking into account the relevant signal characteristics.
- This study presents an experimental investigation of the impact of low sampling rates on transient-based RF fingerprinting, specifically employing a low-cost receiver.
- The impact of the duration of the transient-based identification signal at various sampling rates on the classification performance is presented.

The rest of this paper is organized as follows. Section 2 describes the fingerprinting system. Section 3 presents the experimental setup. In Section 4, the design of the receiver filter chain in the SDR receiver is described. Experimental results are given in Section 5. Section 6 concludes the paper.

2. RF Fingerprinting System

The block diagram of the RF fingerprinting system considered in this work is given in Figure 1. In the data acquisition stage, Wi-Fi signals are captured using a low-cost SDR receiver, operating at low sampling rates. We design the receiver filter chain in the SDR, as explained in Section 4, considering the properties of Wi-Fi signals. After data acquisition, transient signals at the beginning of each Wi-Fi packet are detected in the detection stage. Features are extracted from detected signals and applied to a classifier. Details of the methods used in transient detection, feature extraction, and classification stages are given in the remaining part of this section.

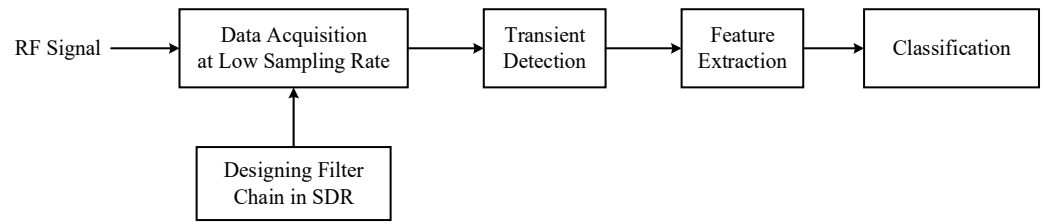


Figure 1. Block diagram of the RF fingerprinting system containing the design of receiver filter chain.

RF signals are down-converted and digitized using an SDR receiver that has a zero intermediate frequency (IF) receiver architecture. By using the in-phase, $x_I[n]$, and quadrature, $x_Q[n]$ signals obtained from the SDR receiver, a complex baseband signal centered at zero frequency is formed as follows:

$$x[n] = x_I[n] + jx_Q[n] \quad (1)$$

Instantaneous amplitude values of the complex baseband signal, given in Figure 2, are usually utilized for RF fingerprinting purposes, which are calculated as

$$a[n] = \sqrt{x_I^2[n] + x_Q^2[n]} \quad (2)$$

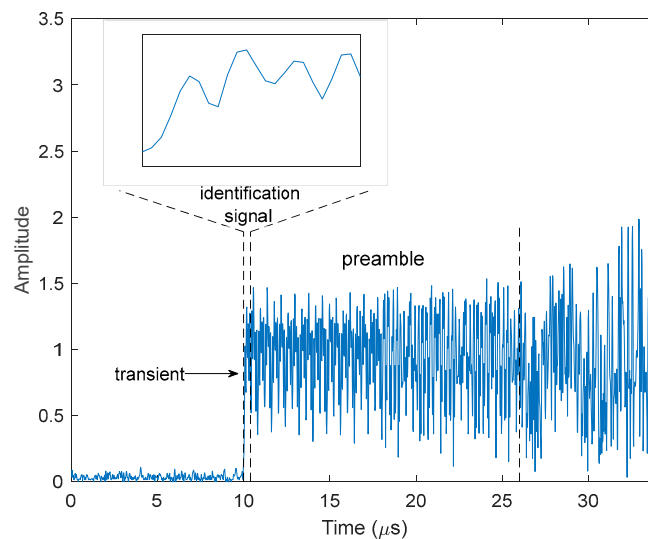


Figure 2. Instantaneous amplitude values of a captured Wi-Fi signal.

In the detection stage, transient signals are detected and their arrival times are estimated. Wi-Fi transmitters emit signals, having transient characters at the start of each packet until they increase the power up to a certain level. Accurately detecting transient signals and determining their starting points is a challenging problem due to the non-stationary nature of these signals. However, the success of this task directly affects the performance of the overall system. In this study, a robust transient detection method [23], which is based on a generalized likelihood ratio algorithm, is employed. In this method, after detecting the transients, the starting points of these signals are estimated within an abrupt change detection framework. Since the signals we are analyzing are sampled at low rates, the transition from channel noise to signal appears as an abrupt change, making this method suitable for our purposes.

In this method, detection is performed by identifying a change in the parameters of the instantaneous amplitudes $a[n]$ of the signals. They are taken as a sequence of independent

Gaussian random variables with different parameters before and after the change point. A recursive decision function is defined as:

$$g[n] = \max\{0, g[n-1] + L[n]\} \quad (3)$$

where n is the current time index and $L[n]$ is the log-likelihood ratio with the model parameters before and after the change point.

$$L[n] = \ln \frac{p(x[n-W+1]; \hat{\theta}_1[n])}{p(x[n-W+1]; \hat{\theta}_0[n])} \quad (4)$$

where $\hat{\theta}_0[n] = (\hat{\mu}_0[n], \hat{\sigma}_0^2[n])$ and $\hat{\theta}_1[n] = (\hat{\mu}_1[n], \hat{\sigma}_1^2[n])$ are the estimated parameters before and after the change point, respectively, and W is the size of the sliding test window that is used for obtaining $\hat{\theta}_1[n]$. $\hat{\mu}_{0,1}[n]$ and $\hat{\sigma}_{0,1}^2[n]$ are the sample mean and the sample variance, respectively, and the methodology employed for estimating these parameters is detailed in [23].

By estimating the model parameters, the decision function is calculated for each observation and compared with a threshold. After detection is performed, which means the decision function exceeds the threshold, the transient starting point is estimated by calculating:

$$\operatorname{argmin}_i \{S[i]\} - W + 1 \quad (5)$$

where i denotes the index of the sample being tested as a possible change point and is limited with the time instant that the decision function exceeds the threshold. $S[i]$ is the cumulative sum of log-likelihood ratios, calculated as:

$$S[i] = \sum_{j=1}^i L[j] \quad (6)$$

Since there may be different transient durations among the various transmitters operating in the same transmission standard [4,6], determining a single duration is challenging. In the literature, there are studies that determine the duration by visual inspection [3] or through an empirical approach [6]. In this study, we use identification signals that contain transients and have a constant length determined experimentally. We refer to these signals as transient-based identification signals, which are considerably shorter in duration compared to preamble signals, as seen in Figure 2.

Instantaneous amplitude values of transient-based identification signals are used as features since they carry characteristic information that can be utilized for device classification. In order to mitigate the influence of signal power on classification performance, these features are normalized as follows:

$$F[n] = \frac{a[n]}{\sqrt{P}} \quad (7)$$

where P is average signal power. Features are classified through a classifier based on probabilistic neural network [24], in which a Parzen window approach is used to estimate the distribution of each class during the training phase. In the testing step, the new input data are assigned to the class that have the highest posterior probability.

3. Experimental Setup

In the experiments, IEEE 802.11n signals were captured in wireless conditions from 20 Wi-Fi transmitters operating on a 20 MHz channel using a software-defined radio (SDR),

which are shown in Figure 3. The transmitters were connected to USB hubs. The positions of these hubs and the SDR receiver were fixed and located 3 m apart from each other, maintaining a line-of-sight. The SDR receiver, Analog Devices ADALM Pluto [25], has a zero-IF receiver architecture and is used to capture in-phase and quadrature baseband signals at different sampling rates of 20 MS/s, 25 MS/s, 40 MS/s, and 60 MS/s. In a zero-IF receiver, the baseband bandwidth is half of the RF channel bandwidth [26]. Therefore, for the 802.11n transmissions with a 20 MHz channel bandwidth examined in this study, the baseband bandwidth is 10 MHz. In this case, the Nyquist sampling rate is 20 MS/s, and 25 MS/s corresponds to the commonly used value of 2.5 times the baseband channel bandwidth in practice. The value of 60 MS/s was chosen as close to the maximum sampling rate of the SDR, i.e., 61.44 MS/s. Thus, the classification performance of transient-based RF fingerprinting was investigated at sampling rates in the order of MS/s as well as close to the Nyquist limit.



Figure 3. SDR receiver (left) and IEEE 802.11 transmitters (right).

A total of 6000 signals were collected for each sampling rate by obtaining 300 samples from each of 20 Wi-Fi transmitters operating in IEEE 802.11n with a bandwidth of 20 MHz. The details about the Wi-Fi transmitters are given in Table 1. The receiver gain was adjusted to two different levels to capture the signals with different SNR values. The average SNR levels across all transmissions were calculated as 30 dB for high receiver gain. For low receiver gain, the calculated SNR was 15 dB, which is the minimum SNR needed to support many wireless local area network applications in practice [27].

Table 1. IEEE 802.11 transmitters used for the experiments.

Model	Chipset	Quantity
TP-Link WN722N	Realtek RTL8188EUS	13
TP-Link WN725N	Realtek RTL8188EUS	3
Mercusys MU6H	Realtek RTL8811CU	2
Mercusys MW150US	Realtek RTL8188EU	2

4. Designing Filter Chain in SDR Receiver

In an SDR receiver, the RF signal is down-converted to the baseband with the I/Q mixer and then passed through a receiver filter chain, consisting of analog and digital filters, on the transceiver chip [28]. The receiver filter chain provides anti-aliasing, bandwidth limiting, and out-of-band rejection. Although these filters have default settings, configuring the filters in accordance with the characteristics of specific applications, the properties of the transmitted signal, and the conditions of environment is essential in order to obtain the expected outcomes while working with real life scenarios [29].

For the ADALM Pluto SDR employed in this work, the receiver filter chain of AD9363 transceiver chip [26] can be used with default settings. However, the default filter chain

may not satisfy the specific requirements of the application, in which case a custom filter can be designed by taking into account the specific requirements of the application [30]. Since our main aim is to extract fingerprints carrying characteristic information about the wireless transmitters, we need to focus on the spectrum of transmitted signals to obtain the distinctive features with minimal distortion. Therefore, a custom filter chain was designed to retain the spectrum of the desired signals as much as possible while at the same time rejecting signals in adjacent channels as well as the out-of-band noise.

Parameters of the custom filter chain were determined considering the transmit spectrum mask for the orthogonal frequency division multiplexing (OFDM) physical layer defined by IEEE 802.11 standard for Wi-Fi transmitters [31]. According to the regulatory restrictions, for the channel bandwidth of 20 MHz, the transmitted spectrum must have a 0 dB (dB relative to the maximum spectral density of the signal) bandwidth that does not exceed 18 MHz [31]. Additionally, the transmitted spectrum must have -20 dB, -28 dB, and -40 dB at frequency offsets of 11 MHz, 20 MHz, and 30 MHz or greater, respectively. Hence, in practice, interference with adjacent channels is mitigated by designing Wi-Fi transmitters with output filters that have a high roll-off.

Because of the restrictions imposed on the output power of transmitters, spectral components outside the transmission bandwidth will be significantly attenuated. Extracting RF fingerprints from outside the transmission bandwidth may become impractical due to background noise and signals in adjacent channels. Therefore, filter chain parameters were determined by considering transmitted spectrum. RF bandwidth was set as close as possible to 18 MHz, which is 0 dB bandwidth of Wi-Fi transmitters, and the bandwidth of the analog low-pass filter was defined accordingly. An FIR filter was designed with a passband frequency of 9 MHz and a stopband frequency of 11 MHz. The design of the receiver filter chain of AD9363 was performed using the MATLAB application developed by Analog Devices [28,32]. The designed filter characteristics for a sampling rate of 40 MS/s are shown in Figure 4. The designed filter chain is separately applied to real-valued in-phase and quadrature signals obtained from the SDR receiver. The results of classification performance for Wi-Fi signals obtained by using both default and designed filter chains are presented in Section 5.2.

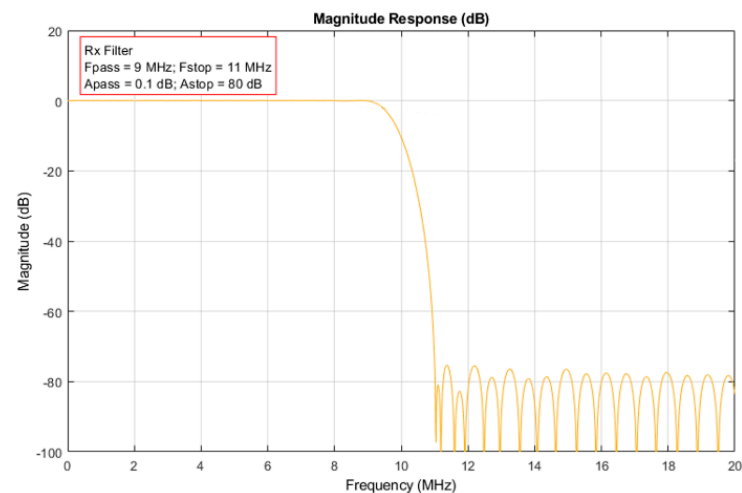


Figure 4. Overall characteristic of the designed filter chain for sampling rate of 40 MS/s.

5. Experimental Results

The effects of the receiver filter chain, sampling rate, and identification signal duration on classification performance were examined using experimental data. This section first describes the design of the receiver filter chain and then shows its impact on classification

performance, comparing the performance of the designed filter with that of the default filter to demonstrate its effectiveness.

5.1. Effects of Receiver Filter Chain on the Signal Spectrum

In order to see the effects of the default and designed filters on the spectrum of the received signals, power spectral densities of the signals obtained by using the corresponding filters at sampling rates of 20 MS/s and 40 MS/s are given in Figures 5 and 6. As illustrated in Figure 5a,b, the default filter chain distorts the spectral components of the signal near the bandwidth edges at a sampling rate of 20 MS/s, while inadequately filtering the out-of-band components at a sampling rate of 40 MS/s. On the other hand, for the designed filter, the desired signal spectrum is obtained without distortion and with significant attenuation of out-of-band components for both sampling rates, as shown in Figure 6a,b.

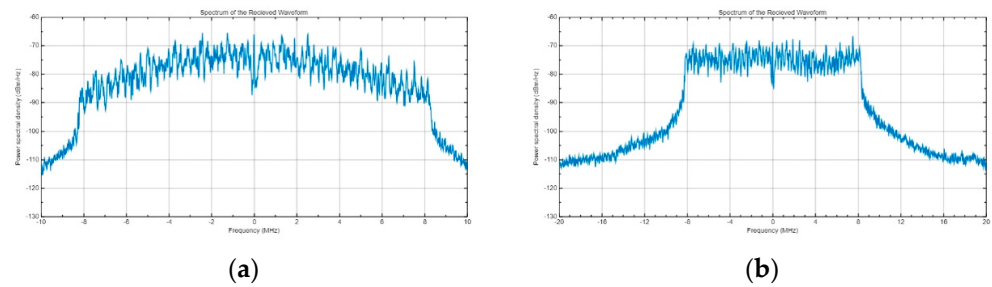


Figure 5. Power spectral densities of signals obtained using the default filter chain for sampling rates of (a) 20 MS/s and (b) 40 MS/s.

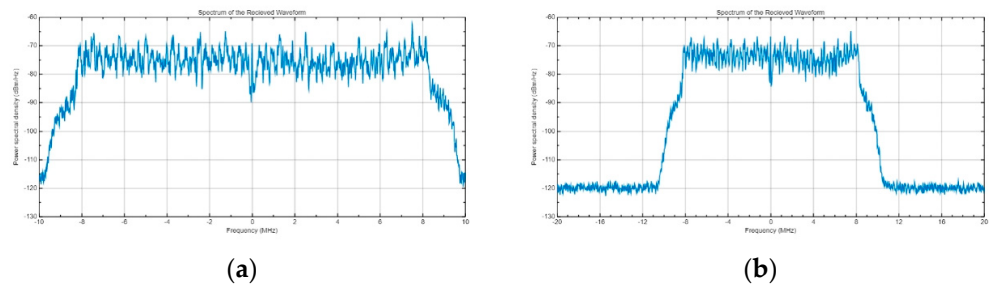


Figure 6. Power spectral densities of signals obtained using the designed filter chain for sampling rates of (a) 20 MS/s and (b) 40 MS/s.

As seen in Figure 5, since the default settings of the receiver filter chain are based on the baseband sampling rate [30], as the sampling rate increases, the overall filter bandwidth of the default filter chain is broadened; conversely, a decrease in the sampling rate will result in a narrower bandwidth of the default filter chain. Note that the frequency ranges are not identical in the figures. Specifically, as the sampling rate decreases further, approaching the Nyquist sampling rate, the bandwidth of the filter becomes narrower than the signal's bandwidth, which will cause distortions on the spectral components of the signal, as seen in Figure 5a. This distortion cannot be compensated even with post-collection signal processing. In addition, out-of-band components cannot be adequately filtered out because the default filter bandwidth broadens as the sampling rate increases.

On the other hand, as seen in Figure 6a,b, the designed filter chain retains the spectral components of the desired signal as much as possible while providing a high out-of-band rejection. Unlike the default filter chain, which is set according to the baseband sampling rate, our designed filter chain is configured according to the bandwidth of the transmitted IEEE 802.11n signals. Therefore, as the sampling rate changes, except for the insignificant variations due to the clock rate and decimation factor, the overall filter characteristic remains almost constant.

Comparing Figures 5b and 6b, although the signals obtained using the designed and the default filter have the same bandwidths, the corresponding filters have different attenuation rates outside the passband. Specifically, at an offset value of 12 MHz from the center frequency, the power spectral densities of the signals obtained using the default filter and the designed filter are approximately -103 dBm/Hz and -120 dBm/Hz, respectively. The designed filter provides a high out-of-band rejection that results in higher attenuation outside the transmission bandwidth. Therefore, decreasing the distorting effects of the out-of-band noise will prevent the RF fingerprints being distorted.

5.2. Classification Performance Results

Evaluating the performance of transient-based RF fingerprinting relies on classification tests conducted using a Monte Carlo cross-validation approach, which consists of 100 trials. In each trial, 80% of the fingerprints extracted from 300 signals for each transmitter were randomly selected to form the training set, while the remaining fingerprints were used for testing. Normalized instantaneous amplitude values of transient-based identification signals, given in (7), were used as features. RF fingerprints consisting of these features were classified using a classifier based on probabilistic neural network, as explained in Section 2. The classification performance presented in this section were obtained by averaging the results of the trials.

The classification accuracy is defined as the ratio of correctly classified signals to the total number of signals in the test set. In each classification test, 20% of the 300 signals collected from each of the 20 Wi-Fi transmitters, a total of 1200 unknown test signals, were classified.

Comparisons of the classification results for default and designed receiver filter chains for both collected SNR values of 15 dB and 30 dB are given in Figures 7a and 7b, respectively. For the default filter, performance degrades both at low and high sampling rates, especially at low SNR. For low sampling rates, as previously mentioned, the filter bandwidth becomes narrower. So, the distinctive information that can be obtained from the identification signals is lost. On the other hand, for high sampling rates, the filter bandwidth becomes broadened, increasing the out-of-band noise that distorts the RF fingerprints. For the high SNR value, the distinctive information is more likely to be preserved, resulting in lower performance degradation.

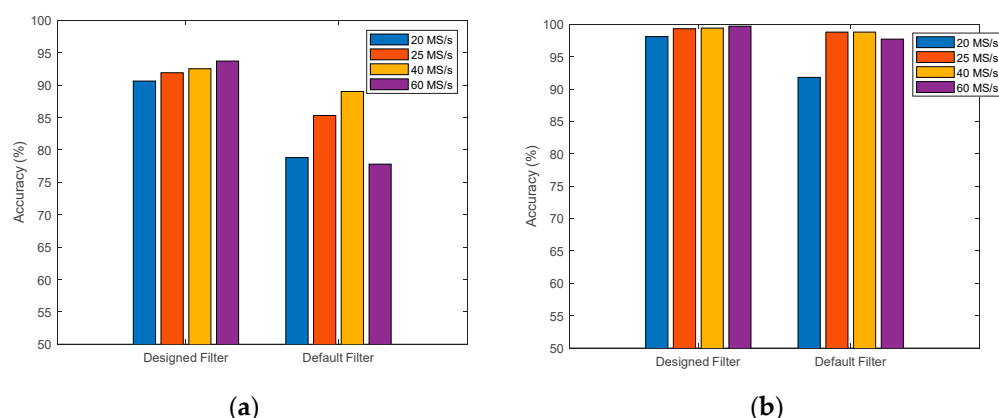


Figure 7. The classification performance results for the designed and default filter chains for SNR values of (a) 15 dB and (b) 30 dB.

With proper filter design according to the IEEE 802.11n signals, the classification performance is superior to that of the default filter chain at all sampling rates for both SNR levels. This result shows that the proper filter design prevents distortion on RF fingerprints. The performance improvement achieved with the designed filter is remarkable at the lower

SNR value, as seen in Figure 7a. With the designed filter, classification accuracies are approximately 92% and 99% at sampling rates exceeding 2.5 times the baseband bandwidth for SNR values of 15 dB and 30 dB, respectively.

The improvement in classification performance achieved by using the designed receiver filter chain, as compared to the default filter, for both 15 dB and 30 dB SNR values is presented in Table 2. There is an improvement in classification accuracy for both SNR values, with a particularly significant improvement observed at 15 dB SNR, highlighting the importance of proper filter design, especially for low SNR values.

Table 2. The improvement in classification performance achieved by using the designed receiver filter chain, as compared to the default filter.

SNR	20 MS/s	25 MS/s	40 MS/s	60 MS/s
15 dB	15.0%	7.7%	3.9%	20.4%
30 dB	6.9%	0.5%	0.6%	2.0%

To evaluate the impact of sampling rate, the variation in classification performance relative to the Nyquist limit at different sampling rates for the designed and the default filters is presented in Table 3. Changing the sampling rate for the default filter directly affects classification performance; in fact, performance can be even worse than what is observed at the Nyquist limit. On the other hand, the impact of the sampling rate is negligible when using the designed receiver filter chain, indicating that high performance can be achieved using low-cost receivers operating at low sampling rates.

Table 3. The variation in classification performance relative to the Nyquist limit at different sampling rates.

Sampling Rate	Designed Filter		Default Filter	
	30 dB SNR	15 dB SNR	30 dB SNR	15 dB SNR
25 MS/s	1.2%	1.4%	7.6%	8.2%
40 MS/s	1.3%	2.1%	7.6%	12.9%
60 MS/s	1.6%	3.4%	6.4%	−1.3%

While utilizing the designed filter chain in the SDR receiver, the classification results obtained for different sampling rates and identification signal durations are presented in Figures 8 and 9 for 15 dB and 30 dB, respectively. Extending the identification signal duration to a certain value substantially enhances classification performance for all sampling rates; however, no significant improvement is observed when further increases beyond that point are conducted.

For the 15 dB SNR value, when the signal duration exceeds 0.6 μ s, the classification performance reaches approximately 92%, and no significant enhancement is attained for sampling rates greater than 2.5 times the baseband bandwidth, as illustrated in Figure 8. On the other hand, determining an insufficient signal duration results in incomplete capture of the transient signal containing characteristic information, which adversely affects the classification performance. For very short signal durations, increasing the sampling rate improves the classification performance to a certain extent; however, it remains below the achievable level.

For the 30 dB SNR value, as illustrated in Figure 9, classification performance is similarly affected by the sampling rate and signal duration, as observed in the lower SNR scenario. It is evident that a shorter signal duration is sufficient to attain high classification performance at 30 dB SNR. Specifically, with a signal duration of 0.4 μ s, classification

performance approaches 99% across all sampling rates, even at the Nyquist limit. As SNR increases, the duration of the identification signal required to acquire the achievable performance decreases approximately at a ratio of 2/3.

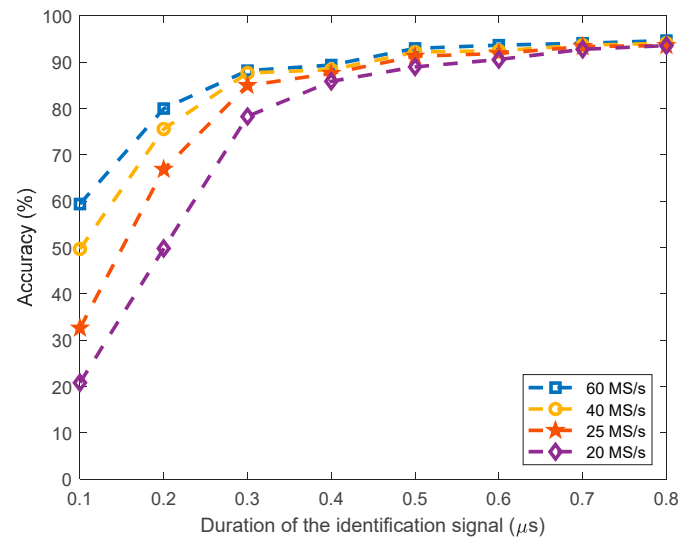


Figure 8. Classification performance results for different sampling rates and identification signal durations for the designed filter at the SNR value of 15 dB.

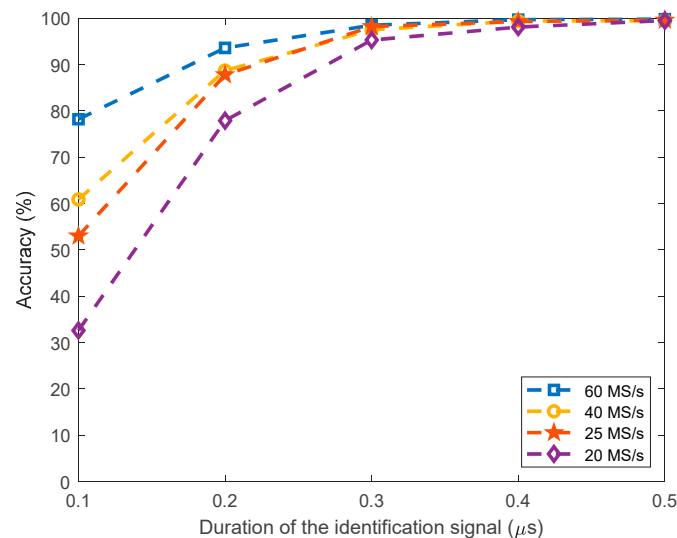


Figure 9. Classification performance results for different sampling rates and identification signal durations for the designed filter at the SNR value of 30 dB.

6. Conclusions

In this paper, we propose designing the filter chain in a low-cost SDR receiver in accordance with the relevant signal characteristics to improve the transient-based RF fingerprinting performance. The designed filter enables both noise reduction and high out-of-band rejection in the data acquisition step. Thus, a high classification performance is achieved at low sampling rates, even close to the Nyquist sampling limit. Experimental results imply that increasing the duration of the transient-based identification signal yields more distinctive information about the transmitters rather than using a high sampling rate, which is simply a cost-effective solution. As a new research topic, comparing the classification performance obtained with different types of SDR receivers using the proposed approach can yield valuable insights. In addition, the impact of radio channels on

classification performance, particularly regarding the effects of transmitter and receiver locations, is considered as a future study.

Author Contributions: Conceptualization, S.T., A.K., M.K. and G.S.; methodology, S.T., A.K. and M.K.; software, S.T., M.K. and G.S.; investigation, S.T., A.K. and M.K.; data curation, S.T., M.K. and G.S.; writing—original draft preparation, S.T. and A.K.; writing—review and editing, A.K., S.T. and G.S.; supervision, S.T. All authors have read and agreed to the published version of the manuscript.

Funding: This work was supported by the Scientific and Technological Research Council of Türkiye (TÜBİTAK) under Grant 119E598.

Data Availability Statement: The datasets presented in this article are not readily available because the data are part of an ongoing study.

Conflicts of Interest: The authors declare no conflicts of interest.

References

1. Atzori, L.; Iera, A.; Morabito, G. The Internet of Things: A survey. *Comput. Netw.* **2010**, *54*, 2787–2805. [[CrossRef](#)]
2. Abbas, S.; Abu Talib, M.; Nasir, Q.; Idhis, S.; Alaboudi, M.; Mohamed, A. Radio frequency fingerprinting techniques for device identification: A survey. *Int. J. Inf. Secur.* **2024**, *23*, 1389–1427. [[CrossRef](#)]
3. Danev, B.; Capkun, S. Transient-Based Identification of Wireless Sensor Nodes. In Proceedings of the 2009 International Conference on Information Processing in Sensor Networks (Ipsn 2009), San Francisco, CA, USA, 13–16 April 2009; pp. 25–36.
4. Rehman, S.U.; Sowerby, K.; Coghill, C. RF Fingerprint Extraction from the Energy Envelope of an Instantaneous Transient Signal. In Proceedings of the 2012 Australian Communications Theory Workshop (AusCTW), Wellington, New Zealand, 30 January–2 February 2012; pp. 90–95.
5. Ureten, O.; Serinken, N. Bayesian detection of Wi-Fi transmitter RF fingerprints. *Electron. Lett.* **2005**, *41*, 373–374. [[CrossRef](#)]
6. Ureten, O.; Serinken, N. Wireless security through RF fingerprinting. *Can. J. Electr. Comput. Eng.* **2007**, *32*, 27–33. [[CrossRef](#)]
7. Huang, R.H.; Peng, X.Y.; Chai, Z.; Li, M.Y.; Ren, J.W.; Yang, X.L. Radio frequency fingerprint extraction and authentication towards open set in noisy channels. *Digit. Signal Process.* **2024**, *146*, 104363. [[CrossRef](#)]
8. Ramsey, B.W.; Stubbs, T.D.; Mullins, B.E.; Temple, M.A.; Buckner, M.A. Wireless infrastructure protection using low-cost radio frequency fingerprinting receivers. *Int. J. Crit. Infrastruct. Prot.* **2015**, *8*, 27–39. [[CrossRef](#)]
9. Rehman, S.U.; Sowerby, K.; Coghill, C. Analysis of Receiver Front End on the Performance of RF Fingerprinting. In Proceedings of the 2012 IEEE 23rd International Symposium on Personal, Indoor and Mobile Radio Communications-(PIMRC), Sydney, Australia, 9–12 September 2012; pp. 2494–2499.
10. Shen, G.X.; Zhang, J.Q.; Marshall, A.; Valkama, M.; Cavallaro, J.R. Toward Length-Versatile and Noise-Robust Radio Frequency Fingerprint Identification. *IEEE Trans. Inf. Forensics Secur.* **2023**, *18*, 2355–2367. [[CrossRef](#)]
11. Zhou, X.Y.; Hu, A.Q.; Li, G.Y.; Peng, L.N.; Xing, Y.X.; Yu, J.B. A Robust Radio-Frequency Fingerprint Extraction Scheme for Practical Device Recognition. *IEEE Internet Things J.* **2021**, *8*, 11276–11289. [[CrossRef](#)]
12. Zhang, B.; Zhang, T.; Ma, Y.Y.; Xi, Z.S.; He, C.; Wang, Y.F.; Lv, Z. A Low-Latency Approach for RFF Identification in Open-Set Scenarios. *Electronics* **2024**, *13*, 384. [[CrossRef](#)]
13. Baldini, G. Enhancement of Transient-Based Radio Frequency Fingerprinting with Smoothing and Gradient Functions. In Proceedings of the 2024 Joint European Conference on Networks and Communications & 6G Summit (EuCNC/6G Summit), Antwerp, Belgium, 3–6 June 2024; pp. 499–504. [[CrossRef](#)]
14. Jagannath, A.; Jagannath, J.; Kumar, P.S.P.V. A comprehensive survey on radio frequency (RF) fingerprinting: Traditional approaches, deep learning, and open challenges. *Comput. Netw.* **2022**, *219*, 109455. [[CrossRef](#)]
15. Soltanieh, N.; Norouzi, Y.; Yang, Y.; Karmakar, N.C. A Review of Radio Frequency Fingerprinting Techniques. *IEEE J. Radio Freq. Identif.* **2020**, *4*, 222–233. [[CrossRef](#)]
16. Uzundurukan, E.; Dalveren, Y.; Kara, A. A Database for the Radio Frequency Fingerprinting of Bluetooth Devices. *Data* **2020**, *5*, 55. [[CrossRef](#)]
17. Tascioglu, S.; Köse, M.; Telatar, Z. Effect of Sampling Rate on Transient Based RF Fingerprinting. In Proceedings of the 2017 10th International Conference on Electrical and Electronics Engineering (Eleco), Bursa, Turkey, 30 November–2 December 2017; pp. 1156–1160.
18. Zhang, S.L.; Huang, W.Q.; Liu, Y.L. A systematic survey on physical layer security oriented to reconfigurable intelligent surface empowered 6G. *Comput. Secur.* **2025**, *148*, 104100. [[CrossRef](#)]
19. Jiang, Q.; Sha, J. RF Fingerprinting Identification in Low SNR Scenarios for Automatic Identification System. *IEEE Trans. Wirel. Commun.* **2024**, *23*, 2070–2081. [[CrossRef](#)]

20. Zhao, C.; Yu, J.; Luo, G.; Wu, Z. Radio Frequency Fingerprinting Identification of Few-Shot Wireless Signals Based on Deep Metric Learning. *Wirel. Commun. Mob. Comput.* **2023**, *2023*, 2132148. [CrossRef]
21. Wang, W.D.; Gan, L. Radio Frequency Fingerprinting Improved by Statistical Noise Reduction. *IEEE Trans. Cogn. Commun. Netw.* **2022**, *8*, 1444–1452. [CrossRef]
22. Xie, L.; Peng, L.; Zhang, J.; Hu, A. Radio frequency fingerprint identification for Internet of Things: A survey. *Secur. Saf.* **2024**, *3*, 2023022. [CrossRef]
23. Tascioglu, S.; Köse, M.; Soysal, G. Sequential Transient Detection for RF Fingerprinting. *Electronics* **2022**, *11*, 3333. [CrossRef]
24. Duda, R.O.; Hart, P.E.; Hart, P.E.; Stork, D.G. *Pattern Classification*; Wiley: Hoboken, NJ, USA, 2001.
25. ADALM Pluto Software Defined Radio. Analog Devices. Available online: <https://www.analog.com/en/design-center/evaluation-hardware-and-software/evaluation-boards-kits/adalm-pluto.html> (accessed on 15 November 2024).
26. *AD9363 Reference Manual UG-1040*; Analog Devices: Wilmington, MA, USA, 2016.
27. Geier, J. *Designing and Deploying 802.11 Wireless Networks: A Practical Guide to Implementing 802.11n and 802.11ac Wireless Networks For Enterprise-Based Applications*; Cisco Press: Indianapolis, IN, USA, 2015.
28. Wiki Analog. MATLAB Filter Design Wizard for AD9361. Available online: <https://wiki.analog.com/resources/eval/user-guides/ad-fmcomms2-ebz/software/filters> (accessed on 15 November 2024).
29. Di, P.; Cozma, A. Four Quick Steps to Production: Using Model-Based Design for Software-Defined Radio Part 3—Mode S Signals Decoding Algorithm Validation Using Hardware in the Loop. *Analog. Dialogue* **2015**, *49*, 1–5.
30. Sampling Rate-Mathworks. Baseband Sampling Rate and Filter Chains. Available online: <https://www.mathworks.com/help/comm/plutoradio/ug/baseband-sampling-rate-and-filter-chains.html> (accessed on 15 November 2024).
31. *IEEE Std 802.11-2016*; IEEE Standard for Information Technology—Telecommunications and Information Exchange between Systems—Local and Metropolitan Area Networks—Specific Requirements—Part 11: Wireless LAN Medium Access Control (MAC) and Physical Layer (PHY) Specifications. IEEE Publisher: Piscataway, NJ, USA, 2021. [CrossRef]
32. Di, P. AD9361 Filter Design Wizard. Available online: <https://www.mathworks.com/matlabcentral/fileexchange/45843-ad9361-filter-design-wizard> (accessed on 15 November 2024).

Disclaimer/Publisher’s Note: The statements, opinions and data contained in all publications are solely those of the individual author(s) and contributor(s) and not of MDPI and/or the editor(s). MDPI and/or the editor(s) disclaim responsibility for any injury to people or property resulting from any ideas, methods, instructions or products referred to in the content.